

# PULSE WAVE PROPAGATION IN LARGE BLOOD VESSELS BASED ON FLUID-SOLID INTERACTIONS METHODS

Tomohiro Fukui<sup>1,†</sup>, Kim H. Parker<sup>2</sup> and Takami Yamaguchi<sup>3</sup>

1. *Department of Mechanical and System Engineering, Kyoto Institute of Technology, Gosityokaido-cho, Matsugasaki, Sakyo-ku, Kyoto 606-8585, Japan.*

<sup>†</sup>*E-mail: fukui@kit.ac.jp*

2. *Physiological Flow Studies Group, Department of Bioengineering, Imperial College, London, SW7 2AZ, United Kingdom.*

3. *Department of Bioengineering and Robotics, Tohoku University, 6-6-01 Aoba-yama, Sendai 980-8579, Japan.*

**Abstract:** Pulse Wave Velocity (PWV) is recognized by clinicians as an index of mechanical properties of human blood vessels. This concept is based on the Moens-Korteweg equation, which describes the PWV in ideal elastic tubes. However, measured PWV of real human blood vessels cannot be always interpreted by the Moens-Korteweg equation because this formula is not precisely applicable to living blood vessels. It is important to understand the wave propagation in blood vessels for a more reliable diagnosis of vascular disease. In this study, we modeled uniform arteries in a three-dimensional coupled fluid-solid interaction computational scheme, and analyzed the pulse wave propagation. A commercial code (Radioss, Altair Engineering) was used to solve the fluid-solid interactions. The governing equations were the compressive Navier-Stokes equations and the equation of continuity for the fluid region, and the equation of equilibrium for the solid region. At the inlet, a steady flow with Reynolds number 1000 was imposed as the basic flow, then a single rectangular pulse with Reynolds number 4000 was imposed upon the basic flow to produce a propagating wave. We compared the PWV values obtained from the computation with those from the Moens-Korteweg equation, and showed the possibility of applying the computational technique to wave propagation analysis in human large arteries.

## 1. Introduction

The diagnosis of cardiovascular disease by measuring pulse wave velocity (PWV) is believed to be a promising technique. The PWV is defined as the velocity of an arterial wall disturbance toward the periphery, which occurs, for example, due to contraction of the ventricle. In general, the PWV is determined by measuring the time delay of the waveforms,  $\Delta t$ , between the two sites with a known distance  $L$ . Therefore,

$$PWV = \frac{L}{\Delta t}. \quad (1)$$

The PWV is believed by clinicians to be increased with the severity of vascular disease such as atherosclerosis [1-3]. The concept for applying the PWV as an index of vascular disease is based on the Moens-Korteweg equation [4], which formulates the PWV of a long straight elastic tube. According to the Moens-Korteweg equation,

$$PWV = \sqrt{\frac{Eh}{2\rho r_i}}, \quad (2)$$

where  $E$  is the Young's modulus of the arterial wall,  $h$  is the wall thickness,  $\rho$  is the blood density, and  $r_i$  is the internal radius of the artery. For thick-walled tubes, the Moens-Korteweg equation has been modified by computing the strain on the middle wall of the tube [5].

$$PWV' = \sqrt{\frac{Eh}{2\rho(r_i + h/2)}}. \quad (3)$$

In the presence of flow, we assume that the wave will be convected with the cross-sectional averaged velocity of the blood [6]. For a thick-walled tube with flow, we therefore use the “modified Moens-Korteweg equation”,

$$PWV'' = \sqrt{\frac{Eh}{2\rho(r_i + h/2)}} + U. \quad (4)$$

where  $U$  is the cross-sectional averaged velocity of the blood. It is recognized that an increased Young's modulus  $E$  will result in an increased PWV. This interpretation, however, is not always applicable to living blood vessels because the Moens-Korteweg equation includes some assumptions that are not valid for human blood vessels. The Moens-Korteweg equation is valid only when an infinitely long, straight and mechanically as well as geometrically homogeneous tube whose wall is very thin is filled with a still, non-viscous fluid. In a real artery, however, the anatomy and the constitution of the blood vessel differ from place to place, therefore, the mechanical properties of the arterial wall depend on its regional position [7]. Moreover, the geometry of the blood vessel is not infinitely long and straight but distributed complicatedly in a three-dimensional space, including many branches, curved regions, and tapering toward the periphery. In addition, the blood is not stationary but flows with its velocity changing in time and space. Hence, the diagnosis of cardiovascular disease by measuring PWV, which relies on the Moens-Korteweg equation, is not correct in the strict sense. The measured PWV of the human blood vessel is a result of several superimposed factors which influence each other, and are not so simple that the Moens-Korteweg equation can be applied. It is necessary to understand the wave propagation in blood vessels so as to make the measurements of the PWV a more reliable diagnosis of vascular disease.

In this study, we modeled uniform arteries in a three-dimensional fully coupled fluid-solid interaction computational scheme, and analyzed the pulse wave propagation. Then we estimated the PWV of long uniform arteries to assess the accuracy of our computation.

## **2. Methods**

Pulse wave propagation can be described as an arterial wall disturbance caused by the ejection of the blood from the heart that propagates mainly toward the periphery. In this study, we imposed a steady flow as the basic flow perpendicular to the cross section of a three-dimensional long straight artery, then, a single pulse was imposed to produce a compression wave, which induced arterial wall displacement that propagated toward the periphery, and assessed the speed of the pulse wave propagation. In the uniform artery study, we compared the PWV values obtained from the computation with those from the Moens-Korteweg equation.

## 2.1 Numerical models

The blood vessels that we are interested in are the relatively large and thick arteries such as the aorta. The internal radius  $r_i$  and the wall thickness  $h$  of the human aorta are approximately 10 mm and 2 mm, respectively. To meet the requirements for “sufficiently long”, the axial length of the model  $L$  was set to 1000 mm, which is 100 times as long as the internal radius of the human aorta. The Young’s modulus of the human aorta has been studied by many researchers [8-10]. We put a special emphasis on the Young’s modulus at zero strain, and the arterial wall of our computation was assumed to be linearly elastic, with density  $\rho^s = 1000 \text{ kg/m}^3$  and Poisson’s ratio  $\nu = 0.45$ . The blood was assumed to be very slightly compressible to stabilize our computation. The density of the blood  $\rho^f$  is taken to be

$$\rho^f = \rho_0^f + \frac{p}{c^2}, \quad (5)$$

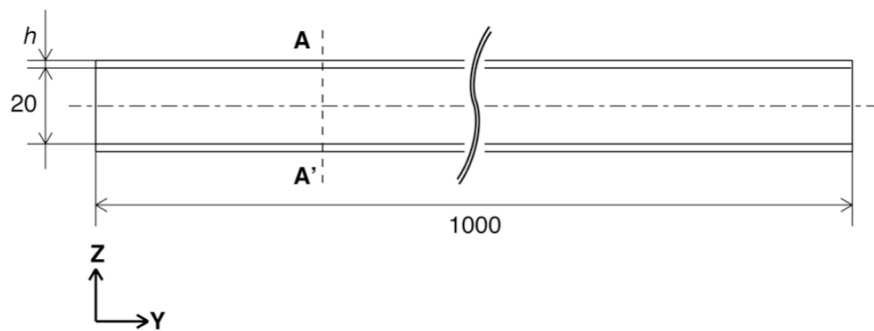
where  $\rho_0^f$  is the initial density,  $p$  is the pressure relating to the external pressure, and  $c$  is the sound speed. This equation shows the relationships between the blood density  $\rho^f$ , the pressure  $p$ , and the sound speed  $c$  due to its compressibility. Higher sound speeds correspond to increased incompressibility of the fluid. The initial density  $\rho_0^f$  was set to  $1000 \text{ kg/m}^3$  and the sound speed  $c$  was to 60 m/s (see discussion below). The viscosity coefficient of the blood  $\mu$  was set to  $4.0 \times 10^{-3} \text{ Pa}\cdot\text{s}$ . The different Young’s moduli of the arterial wall  $E$  and the wall thickness  $h$  used in our calculations are summarized in Table 1; 9 models were used in total.

The cross section of the computational model was defined to be in the Z-X plane, and the Y-axis was in the longitudinal direction of the model. A schematic view of the uniform artery is shown in Fig. 1(a). Figure 1(b) shows one-fourth of the cross sections of the symmetrical model, and the bold line represents the border of the fluid and solid regions. The numbers of elements in one cross section were 476 for the fluid region and 224 for the solid region. The resolution along the longitudinal direction was at 5 mm intervals. The total number of elements in the model, including two extra cross sections at the inlet and the outlet, was 141,400.

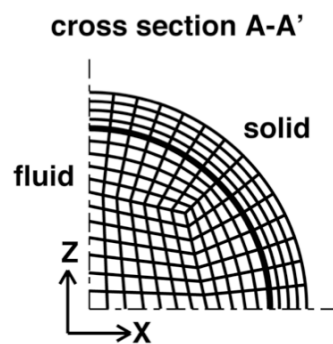
The grids for the solid region, including the border of the fluid and solid regions, were solved by the Lagrangian method in order to adapt for the wall displacement due to the disturbance by the pulse. The grids for the fluid region except for the cells on the fluid-solid border were fixed and solved by the Eulerian method.

**Table 1. Young's modulus and wall thickness of the model uniform artery.**

Young's modulus $E$ (MPa)	0.5	1.0	2.0
Wall thickness $h$ (mm)	1.5	2.0	4.0



(a) Uniform artery model.



(b) Cross section.

**Fig. 1.** Schematic views of the artery models used in this study. (a) shows a uniform artery model, (b) shows one-fourth of the cross sections of the symmetrical model. The bold line in the cross section represents the border of the fluid and solid regions. The number of elements in one cross section; 476 for the fluid, 224 for the solid.

## 2.2 Governing equations and computational code

A commercial code (Radioss, Altair Engineering) was used to solve the fluid-solid interactions with an ALE formulation. The ALE stands for Arbitrary Lagrangian Eulerian, which enables us to solve the interactions with Lagrangian and Eulerian methods arbitrarily. The governing equations for the compressible fluid were the Navier-Stokes equations (Eq. (6)) and the equation of continuity (Eq. (7)).

$$\frac{\partial(\rho^f u_j^f)}{\partial t} + \frac{\partial(\rho^f u_i^f u_j^f)}{\partial x_i} = -\frac{\partial p}{\partial x_j} + \mu \frac{\partial^2 u_j^f}{\partial x_i \partial x_i}, \quad (6)$$

$$\frac{\partial \rho^f}{\partial t} + \frac{\partial(\rho^f u_i^f)}{\partial x_i} = 0, \quad (7)$$

where  $f$  superscribed on the parameters indicates the fluid region,  $\rho^f$  is the fluid density,  $u_i^f$  is the velocity,  $p$  is the pressure, and  $\mu$  is the viscosity coefficient. The equation of equilibrium (Eq. (8)) was solved for the solid wall. The solid was assumed to be a linearly elastic solid (Eq. (9)).

$$\int_V \frac{\partial \sigma_{ij}}{\partial x_j} dV = \int_V \rho^s \frac{\partial u_i^s}{\partial t} dV, \quad (8)$$

$$\sigma_{ij} = C_{ijkl} \varepsilon_{kl}, \quad (9)$$

where  $s$  superscribed on the parameters indicates the solid region,  $\sigma_{ij}$  is the Cauchy stress tensor,  $C_{ijkl}$  is the elastic tensor, and  $\varepsilon_{kl}$  is the strain tensor.

## 2.3 Boundary conditions

The boundary conditions were that both ends of the artery were fixed (Eq. (10)), no-slip on the wall (Eq. (11)), and the ‘silent boundary’ condition which enables us to reduce reflections at the outlet (Eq. (12)).

$$u_i^s = \omega_i^s = 0, \quad (10)$$

$$u_i^f = u_i^s, \quad (11)$$

$$\frac{\partial p}{\partial t} = \rho^f c \frac{\partial u_n^f}{\partial t} + c \frac{(p_\infty - p)}{2l_c}, \quad (12)$$

where  $\omega$  is the angular velocity,  $n$  is the vector perpendicular to the cross section,  $p_\infty$  is the reference pressure, and  $l_c$  is a length characteristic of the grid size. At the inlet, a steady uniform velocity, with Reynolds number 1000 ( $= 0.2$  m/s), perpendicular to the cross section was imposed as the basic flow and computations continued until the initial oscillations of the wall reduced to less than 0.1% of the internal radius of the artery. Then, a single rectangular pulse with a period of 10 ms and the Reynolds number of 4000 ( $= 0.8$  m/s) was imposed upon the basic flow to produce a propagating wave (Fig. 2). The time to establish the basic flow depended on the artery models, however, it was around 10 (s) which is 1000 times as long as that of the single pulse at  $t = 0.0$  (ms). Then, the velocity, displacement, and pressure values were obtained with a sampling rate of 1000 Hz in each model to draw waveforms.

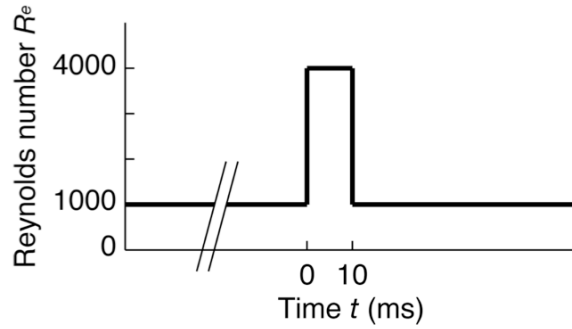


**Fig. 2.** Boundary condition at the inlet. A steady flow was imposed before a single pulse as the basic flow. The time taken to establish the basic flow was around 10 s.

### 3. Results

For the models used in this study, it took about three weeks to finish each calculation with a Linux machine whose processor and memory were 2.4 GHz and 1 GB.

### **3.1 Wave propagation**

Figure 3 shows the color-coded distribution of the axial velocity  $u_y$  in the uniform artery at different times with the Young's modulus of 1.0 MPa and the wall thickness of 2.0 mm at the plane  $x = 0$ . The scale in the radial direction is multiplied by 4 for clarity. The propagation of the velocity pulse towards the periphery is clear.

### **3.2 Velocity waveforms**

The velocity waveforms in the uniform artery were obtained from the axial velocity  $u_y$  on the center-line of the artery. Figure 4 shows the velocity waveforms in the uniform artery with the Young's modulus of 1.0 MPa and the wall thickness of 2.0 mm at  $y = 350, 500, \text{ and } 650$  mm. The peak of the waveform shifted peripherally in time, indicating this wave was forward-going. The PWV was calculated from the estimate of the time delay  $\Delta t$  of each waveform and the distance between the two sites of measurement. This is generally known as the foot-to-foot method [11] since the reference point of the waveform is the foot of each waveform. The foot point was determined by the intersection of the two straight lines; the non-oscillating line before the waveform and the tangential line of the ascending slope. The tangential line was determined to approximate the data between 20 ~ 80% of the ascending slope by least squares. The PWV was then calculated regionally at intervals of 100 mm from  $y = 50 \sim 950$  mm.

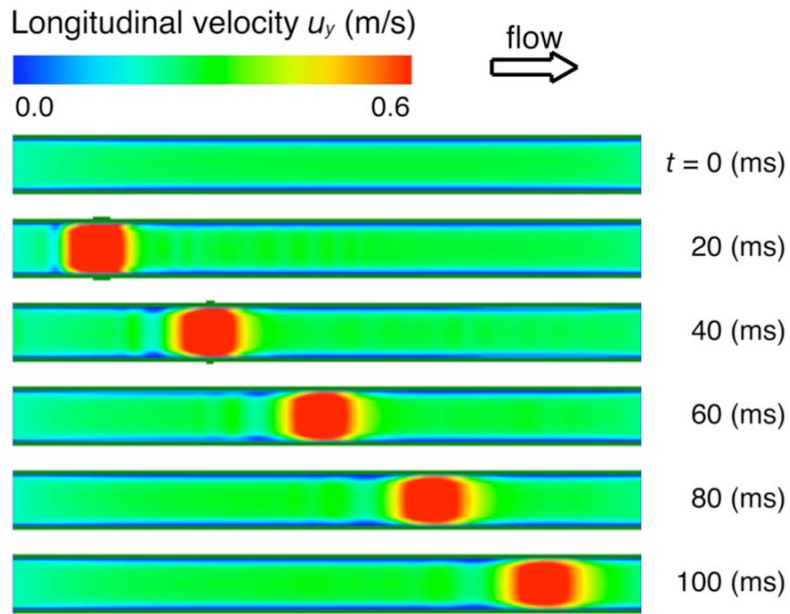


**Fig. 3.** Color-coded distribution of the longitudinal velocity  $u_y$  in the uniform artery with the Young's modulus of 1.0 MPa and the wall thickness of 2.0 mm at the plane  $x = 0$ . The scale in the radial direction is multiplied by 4 for clarity.

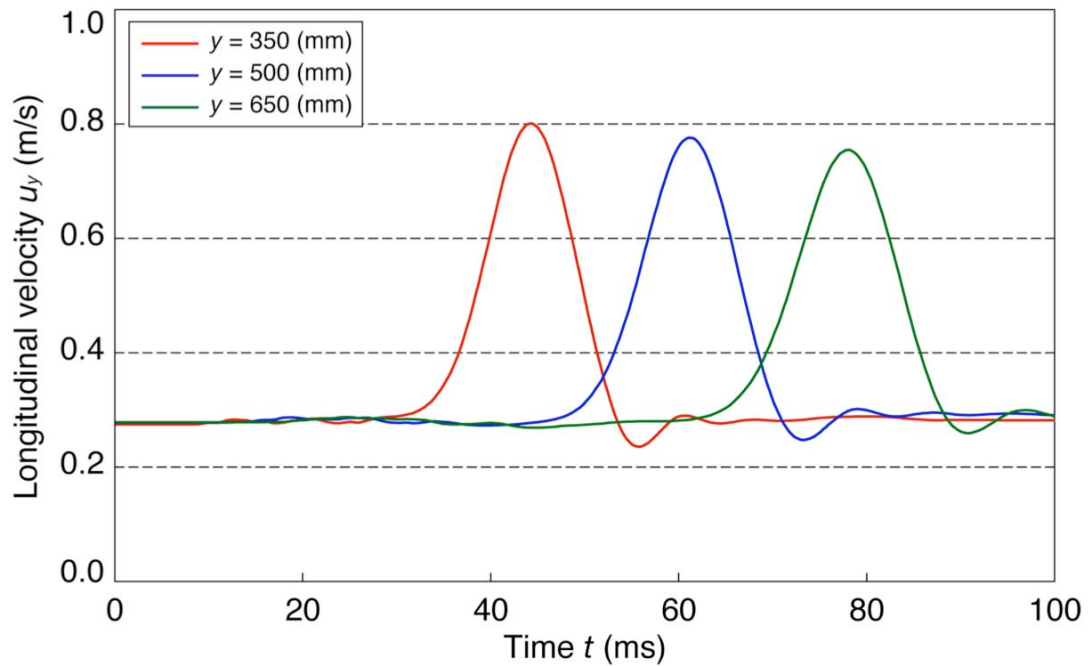


**Fig. 4.** Center-line velocity waveforms at different locations in the uniform artery with the Young's modulus of 1.0 MPa and the wall thickness of 2.0 mm.

### 3.3 Pulse wave velocity

Figure 5 presents the regional PWV of uniform arteries calculated with a Young's modulus of 1.0 MPa. The PWV at  $y = 100$  mm was obtained from the waveforms at  $y = 50$  and 150 mm. The PWV at  $y = 200$  mm was obtained from the waveforms at  $y = 150$  and 250 mm, and so on. The differences in color show the differences in the wall thickness of the artery. The dotted lines show the PWV estimation by the modified Moens-Korteweg equation (Eq. (4)). The averaged velocity over a cross section  $U$  in Eq. (4) was determined with the flow velocity values at  $t = 0.0$  ms. There were good correspondences between the values from the computation and those from the modified Moens-Korteweg equation for the arteries with wall thicknesses of 1.5 and 2 mm. For the artery with a wall thickness of 4 mm, the values were significantly lower than that from the modified Moens-Korteweg equation. There was variation in the PWV values in the longitudinal direction, though, it was less than 10% of the PWV. The larger variation can be seen near both ends. The differences decreased to less than 5% when the PWV values between  $y = 300$  to 700 mm were used.

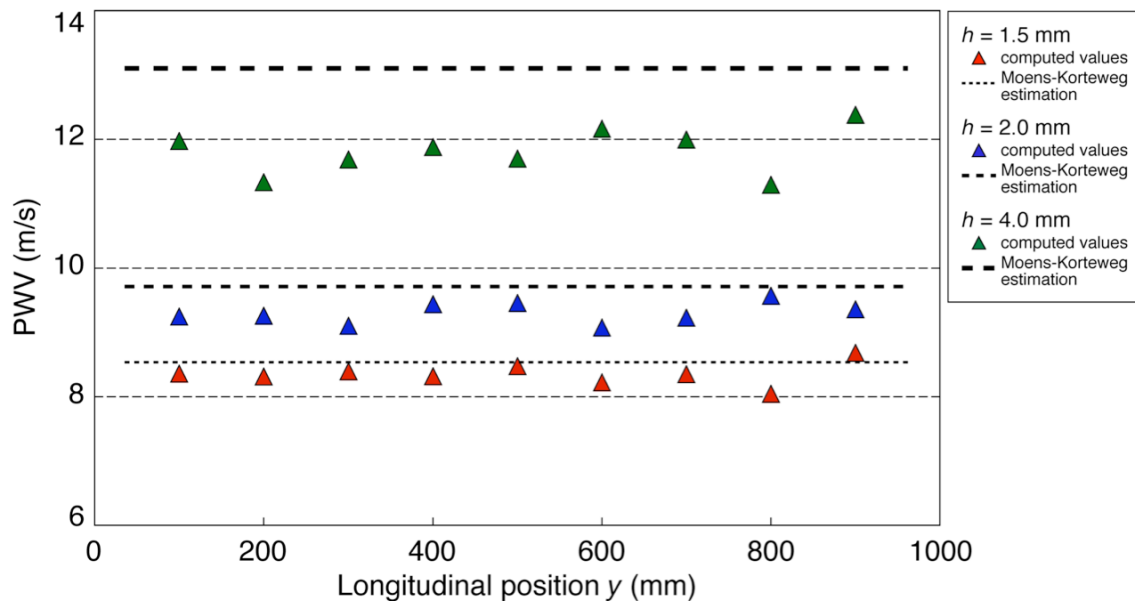


**Fig. 5.** PWV values of the uniform arteries with the Young's modulus of 1.0 MPa in the longitudinal direction. The dotted lines show the PWV estimation by the modified Moens-Korteweg equation.

### 3.4 PWV comparison between computation and theoretical values

The PWV of the nine uniform arteries were estimated, and compared with those from the modified Moens-Korteweg equation (Fig. 6). The ordinate shows the PWV obtained from the computation at the center of the artery,  $y = 500$  mm, and the abscissa shows those from the modified Moens-Korteweg equation (Eq. (4)). The color denotes the wall thickness of the artery and the shape denotes the Young's modulus of the arterial wall. The dotted line indicates the line of equality between the two parameters. The PWV from the computation was lower than those from the modified Moens-Korteweg equation in the higher range of the PWV.

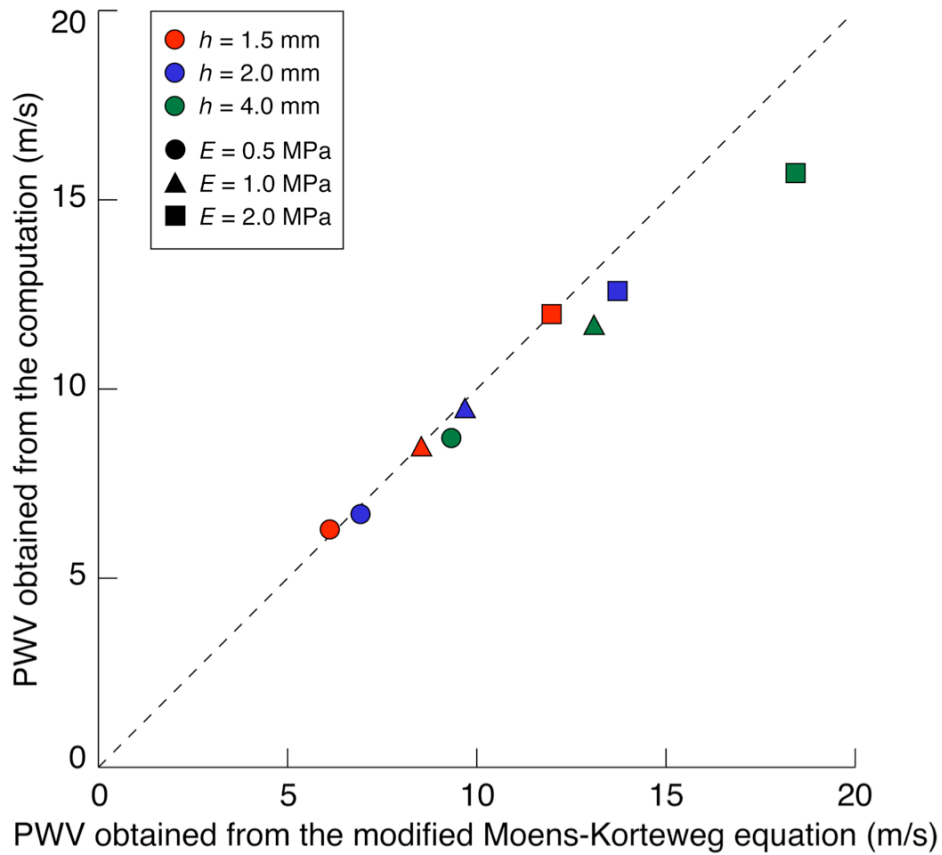


**Fig. 6.** Comparison of the PWV obtained from the computation and those obtained from the modified Moens-Korteweg equation. The dotted line indicates the line of equality between the two parameters.

#### 4. Discussion

As shown in Fig. 5, the PWV values were not constant in the longitudinal direction, but varied by up to 10%. The variation can be seen mainly at both ends and could be attributed to the boundary conditions of our computation. The boundary conditions at both ends were fixed, which means no translating or rotating motions at the ends. Due to the fixed translating motion, the arterial wall at both ends could not be dilated in the radial direction nor elongated in the longitudinal direction. These fixed conditions would produce reflection which could affect the PWV values at the ends. We concluded that when a uniform artery with a length of 1000 mm is used in our computation, the PWV estimation is valid in the center 500 mm of the artery, where the variation of the PWV even for the thickest-walled vessel was less than 5%.

In the higher range of the PWV, the PWV obtained from the computation were lower than those from the modified Moens-Korteweg equation as shown in Fig. 6. One of the reasons for this difference is that the Moens-Korteweg equation is only valid for a cylinder with a very thin wall. The differences between the two parameters were up to 3.9% for the wall thickness of 1.5 mm, up to 8.0% for 2.0 mm, and up to 16.1% for 4.0 mm. The most significant differences can be seen for the wall thickness of 4.0 mm (i.e., 20% of the diameter).

Another reason for the differences in the computation is the inclusion of the sound speed of the blood. The Young's modulus of the arterial wall and the bulk modulus of the blood differ by  $10^3$  to  $10^4$  if the sound speed of the blood is assumed to be the more realistic value of 1500 m/s and the bulk modulus  $K$  can be calculated as  $K = \rho c^2$ . It is impracticable to deal with materials whose elastic modulus differ by  $10^3$  to  $10^4$  with each other for the fluid-solid interaction study with current computer techniques. In this study, therefore, the elastic modulus of the fluid was decreased to the order of that of the solid by assuming the fluid was slightly compressible with the sound speed of 60 m/s. The underestimated PWV of the uniform artery for the higher range of the PWV was attributed to the decreased bulk modulus of the blood. The PWV, which can be expressed as the wave speed due to radial displacement of the arterial wall, never

exceeds the sound wave speed. The higher PWV was more affected by the compressibility of the blood and more underestimated. Nevertheless, the differences between the PWV obtained from the computation and those from the modified Moens-Korteweg equation were less than 7% up to 12 m/s of the PWV, indicating these computational methods for the PWV analysis were accurate enough to evaluate its value quantitatively. Moreover, this range is similar to the PWV of the human aorta, which is our greatest interest. These results show the possibility of applying the computational technique to wave propagation analysis in human large arteries.

## 5. Conclusions

In conclusions, we analyzed the pulse wave propagation with a three-dimensional fluid-solid interaction computational scheme, and showed the possibility of applying the computational technique to wave propagation analysis in human large arteries.

## References:

- [1] Ting CT, Chou CY, Chang MS *et al.* Arterial hemodynamics in human hypertension. Effects of adrenergic blockade. *Circulation* 1991; 84: 1049-1057.
- [2] Lehmann ED, Gosling RG, Sonksen PH. Arterial wall compliance in diabetes. *Diabetic Medicine* 1992; 9: 114-119.
- [3] Triposkiadis F, Kallikazaros I, Trikas A *et al.* A comparative study of the effect of coronary artery disease on ascending and abdominal aorta distensibility and pulse wave velocity. *Acta Cardiologica* 1993; 48: 221-233.
- [4] Bramwell JC, and Hill AV. The velocity of the pulse wave in man. *Proceedings of the Royal Society, London* 1922; B93: 298-306.
- [5] Fung YC. *Biomechanics Circulation*. 2nd ed. New York: Springer 1996.
- [6] Khir AW, O'Brien A, Gibbs JSR, and Paker KH. Determination of wave speed and wave separation in the arteries. *Journal of Biomechanics* 2001; 34: 1145-1155.
- [7] Nakashima T, and Tanikawa J. A study of human aortic distensibility with relation to atherosclerosis and aging. *Angiology* 1971; 22: 477-490.
- [8] MacSweeney ST, Young G, Greenhalgh RM, and Powell JT. Mechanical properties of the aneurysmal aorta. *British Journal of Surgery* 1992; 79: 1281-1284.

- [9] He CM, and Roach MR. The composition and mechanical properties of abdominal aortic aneurysms. *Journal of Vascular Surgery* 1994; 20: 6-13.
- [10] Thubrikar MJ, Labrosse M, Robicsek F, Al-Soudi J, and Fowler B. Mechanical properties of abdominal aortic aneurysm wall. *Journal of Medical Engineering & Technology* 2001; 25: 133-142.
- [11] Khir AW, Zambanini A, and Parker KH. Local and regional wave speed in the aorta: effects of arterial occlusion. *Medical Engineering & Physics* 2004; 26: 23-29.